Novel insights into the taxonomic diversity and molecular mechanisms of bacterial Mn(III) reduction

Nadia Szeinbaum[1,2,6], Brook L. Nunn[3], Amanda R. Cavazos[2], Sean A. Crowe[2,4], Frank J. Stewart[1,5], Thomas J. DiChristina[1], Christopher T. Reinhard[2,6], and Jennifer B. Glass[2,6]*

[1]School of Biological Sciences, Georgia Institute of Technology, Atlanta, GA, USA

[2]School of Earth and Atmospheric Sciences, Georgia Institute of Technology, Atlanta, GA, USA

[3]Department of Genome Sciences, University of Washington, Seattle, WA, USA

[4]Department of Microbiology & Immunology and Department of Earth, Ocean, & Atmospheric Sciences, University of British Columbia, Vancouver, Canada

[5]Department of Microbiology and Immunology, Montana State University, Bozeman, Montana

[6]NASA Astrobiology Institute, Alternative Earths Team, Mountain View, CA

*Corresponding author: jennifer.glass@eas.gatech.edu

Running title: Novel undecaheme in Betaproteobacteria

Originality-Significance Statement: Recent observations suggest that Mn(III)-ligand complexes are geochemically important in diverse aquatic environments. Thus far, microbially-driven Mn(III) reduction has only been associated with *Gammaproteobacteria* encoding three-component outer-membrane porin-cytochrome c conduits. Here, we demonstrate that *Betaproteobacteria* dominate in abundance and with respect to protein expression during biologically-mediated Mn(III) reduction in an enrichment culture from an anoxic lacustrine system. Using metaproteomics, we detect for the first time that *Betaproteobacteria* express a two-component porin-cytochrome c conduit, and an uncharacterized extracellular undecaheme (11-heme) c-type cytochrome. Although this is the first definitive report of an undecaheme within the *Betaproteobacteria,* we find evidence that they are widespread in uncultivated strains. These results widen the phylogenetic diversity of Mn(III)-reducing bacteria, and provide new insights into potential molecular mechanisms for soluble Mn(III) reduction.

Summary: Soluble ligand-bound Mn(III) can support anaerobic microbial respiration in diverse aquatic environments. Thus far, Mn(III) reduction has only been associated with certain *Gammaproteobacteria*. Here, we characterized microbial communities enriched from Mn-replete sediments of Lake Matano, Indonesia. Our results provide the first evidence for biological reduction of soluble Mn(III) outside the *Gammaproteobacteria*. Metagenome assembly and binning revealed a novel betaproteobacterium, which we designate "*Candidatus* Dechloromonas occultata." This organism dominated the enrichment and expressed a porin-cytochrome c complex typically associated with iron-oxidizing *Betaproteobacteria* and a novel cytochrome c-rich protein cluster (Occ), including an undecaheme putatively involved in extracellular electron transfer. This *occ* gene cluster was also detected in diverse aquatic bacteria, including uncultivated *Betaproteobacteria* from the deep subsurface. These observations provide new insight into the taxonomic and functional diversity of microbially-driven Mn(III) reduction in natural environments.

Introduction. Manganese(III) is a strong oxidant with a reduction potential close to molecular oxygen (Kostka et al., 1995). Mn(III) is short-lived and unstable, but its stability is greatly increased when bound to ligands (Luther III et al., 2015). Ligand-bound Mn(III) is often the most abundant dissolved Mn species in sediment porewaters (Madison et al., 2013; Oldham et al., 2019) and soils (Heintze and Mann, 1947), with the potential to facilitate one-electron redox reactions in a variety of biogeochemical cycles (Luther III et al., 2015). Microbes accelerate the oxidation and reduction of Mn by orders of magnitude compared to abiotic mechanisms (Hem, 1963; Diem and Stumm, 1984; Morgan, 2005; Tebo et al., 2005; Learman et al., 2011; Luther et al., 2018; Jung et al., 2020). Yet, despite clear evidence for the environmental importance of Mn(III), knowledge about microbial Mn(III) cycling pathways remains fragmented.

To date, only *Shewanella* spp. (*Gammaproteobacteria*) have been confirmed to respire soluble Mn(III) (Kostka et al., 1995; Szeinbaum et al., 2014). *Shewanella* respire Mn(III) using the Mtr pathway (Szeinbaum et al., 2017), a porin-cytochrome (PCC) conduit that transports electrons across the periplasm for extracellular respiration of Mn(III/IV), Fe(III), and other metals (Richardson et al., 2012; Shi et al., 2016). Many Fe(II)-oxidizing *Betaproteobacteria* also contain PCCs (MtoAB, generally lacking the C subunit), which are proposed to oxidize Fe(II) to Fe(III) by running the PCC in reverse (Emerson et al., 2013; Kato et al., 2015; He et al., 2017). In some metal-reducing *Gammaproteobacteria* and *Deltaproteobacteria*, extracellular undecaheme (11-heme) UndA is thought to play a key functional role in soluble Fe(III) reduction (Fredrickson et al., 2008; Shi et al., 2011; Smith et al., 2013; Yang et al., 2013). UndA's crystal structure shows a surface-exposed heme surrounded by positive charges, which may bind negatively-charged soluble iron chelates (Edwards et al., 2012). Environmental omics suggest that metal reduction by *Betaproteobacteria* may be widespread in the deep subsurface

(Anantharaman et al., 2016; Hernsdorf et al., 2017). However, only a few Fe(III)-reducing *Betaproteobacteria* isolates have been characterized to date (Cummings et al., 1999; Finneran et al., 2003), and little is known about metal reduction pathways in *Betaproteobacteria*.

Manganese reduction coupled to methane (CH_4) oxidation is a novel metabolism only recently discovered in cultures enriched in Archaea (Ettwig et al., 2016; Leu et al., 2020). Biological and geochemical evidence suggest that this metabolism may be found in a variety of environments (Beal et al., 2009; Crowe et al., 2011; Riedinger et al., 2014), including Fe-rich Lake Matano, Indonesia. In an attempt to explore whether CH_4 can fuel microbial Mn(III) reduction in enrichments inoculated with sediments from Lake Matano, Indonesia, which has active and pronounced microbial Mn and CH_4 cycles (Jones et al., 2011), we uncovered a novel betaproteobacterium as the most dominant and active member of our Mn(III)-reducing enrichment culture. Our results provide the first evidence for biological reduction of soluble Mn(III) outside *Gammaproteobacteria* and provide evidence for a new biochemical pathway involved in extracellular electron transfer.

Results and discussion

Enrichment of Mn(III)-reducing populations. Lake Matano, Indonesia, is a permanently stratified ultraoligotrophic lake (Crowe et al., 2008). Below its oxic surface waters, Lake Matano's permanently anoxic and stratified waters are highly enriched in iron and manganese, and support the activity of Mn cycling organisms with organic carbon and CH_4 as potential sources of electrons (Crowe et al., 2011; Jones et al., 2011; Kuntz et al., 2015; Sturm et al., 2019). We designed an enrichment strategy to select for microbes capable of anaerobic CH_4 oxidation coupled to soluble Mn(III) reduction by incubating anoxic Lake Matano sediment

communities with soluble Mn(III)-pyrophosphate as the electron acceptor (with 2% O_2 in a subset of bottles), and CH_4 as the sole electron donor and carbon source after pre-incubation to deplete endogenous organic carbon (see **Supporting Information** for enrichment details). Enrichment cultures were transferred into fresh media after Mn(III) was completely reduced to Mn(II), for a total of five transfers over 395 days. By the fourth transfer, cultures with CH_4 headspace (with or without 2% O_2) reduced ~80% of soluble Mn(III) compared to ~30% with N_2 headspace (**Fig. 1**). 16S rRNA gene sequences were dominated by *Betaproteobacteria* (*Rhodocyclales*; 8-35%) and *Deltaproteobacteria* (*Desulfuromonadales*; 13-26%; **Fig. S1)**. $^{13}CH_4$ oxidation to $^{13}CO_2$ was undetectable (**Fig. S2**).

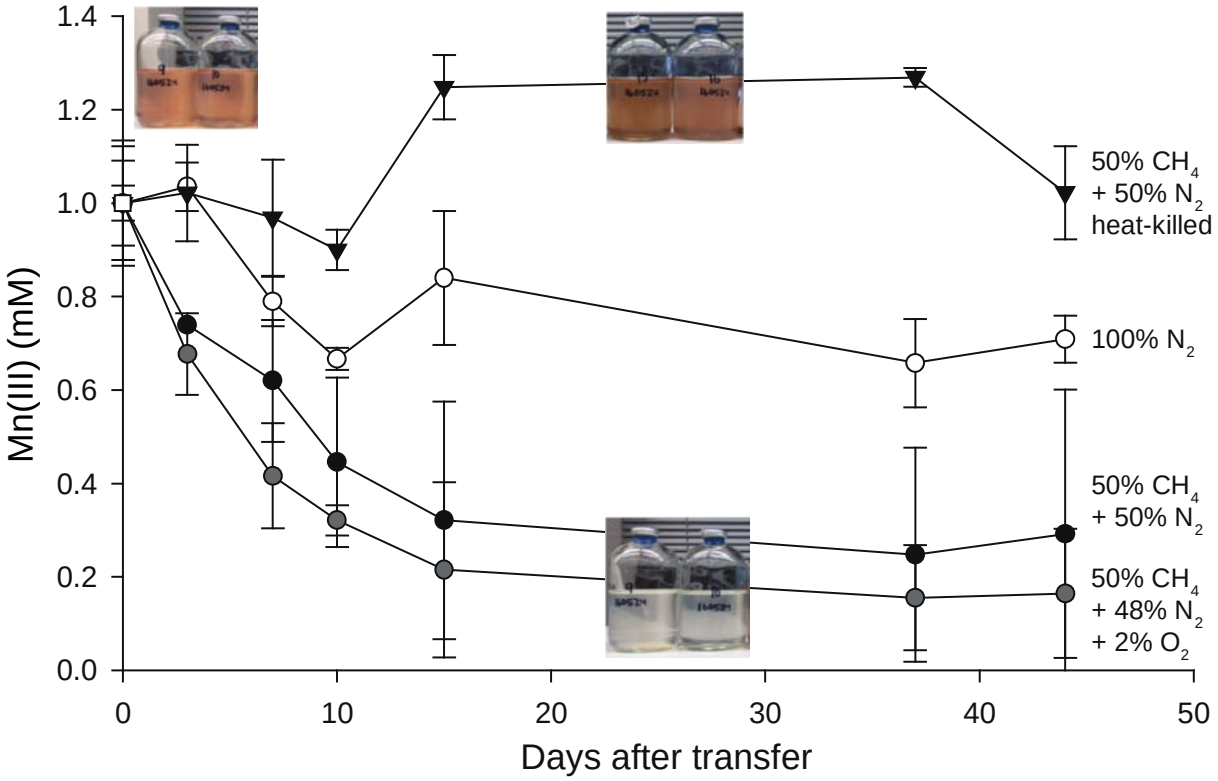

Figure 1. Consumption of Mn(III) in Lake Matano enrichments in the presence and absence of methane. Sediment-free cultures (transfer 4), from 335 days after the initial enrichment, were incubated for 45 days with 1 mM Mn(III) pyrophosphate as the sole electron acceptor. One set was incubated with Mn(III) and 2% O_2. Initial bottle headspace contained 50% CH_4 + 50% N_2 (black circles), 50% CH_4+48% N_2+2% O_2 (gray circles), 100% N_2 (white circles), and 50% CH_4+50% N_2 heat killed controls (black triangles). Error bars are standard deviations from duplicate experiments. Color change from red to clear indicates Mn(III) reduction.

Samples for metagenomic and metaproteomic analysis were harvested from the fifth transfer (**Fig. 1; Fig. S1**). Out of 2,952 proteins identified in the proteome, 90% were assigned to *Betaproteobacteria*; of those, 72% mapped to a 99.5% complete metagenome-assembled genome (MAG; *Rhodocyclales* bacterium GT-UBC; NCBI accession QXPY01000000) with 81-82% average nucleotide identity (ANI) and phylogenetic affiliation to *Dechloromonas* spp. (**Table S1; Fig. S3**). This MAG is named here "*Candidatus* Dechloromonas occultata" sp. nov.; etymology: occultata; (L. fem. adj. 'hidden'). The remaining 10% of proteins mapped to *Deltaproteobacteria*; of those, 70% mapped to a nearly complete MAG (*Desulfuromonadales* bacterium GT-UBC; NCBI accession RHLS01000000) with 80% ANI to *Geobacter sulfurreducens*. This MAG is named here "*Candidatus* Geobacter occultata".

Cytochrome expression during Mn(III) reduction. Cytochromes containing multiple *c*-type hemes are key for electron transport during microbial metal transformations, and therefore also expected to play a role in Mn(III) reduction. Numerous mono-, di-, and multi (>3)-heme cytochromes (MHCs) were expressed by "*Ca.* D. occultata" in Mn(III)-reducing cultures. Nine out of 15 MHCs encoded by the "*Ca.* D. occultata" MAG were expressed, including two decahemes similar to MtoA in Fe(II)-oxidizing *Betaproteobacteria* (**Tables 1, S2, S3; Figs. 2A, S4).** Several highly expressed MHCs were encoded on a previously unreported 19-gene cluster with 10 cytochrome-*c* proteins, hereafter *occA-S* (**Table 1; Figs. 2B, S5, S6**). OccP was predicted to be an extracellular undecaheme protein of ~100 kDa (922 amino acids). "*Ca.* Dechloromonas occultata" may reduce Mn(III) using the novel extracellular undecaheme OccP as the terminal Mn(III) reductase. Experimental verification of the function of the putative Occ complex is currently limited by the scarcity of genetically tractable *Betaproteobacteria.*

Proteins with 40-60% identity to the expressed "*Ca.* D. occultata" OccP protein were widely distributed in *Betaproteobacteria* from diverse freshwaters and deep subsurface groundwaters, as well as in several *Gammaproteobacteria* and one alphaproteobacterium (**Fig. 2D; Table S3).** Most *occP*-containing bacteria also possessed *mtoA* and denitrification genes (**Fig. 2D**; **Figs. S7**, **S8)**. These results widen the phylogenetic diversity of candidate extracellular MHCs that may be involved in microbial Mn(III) reduction.

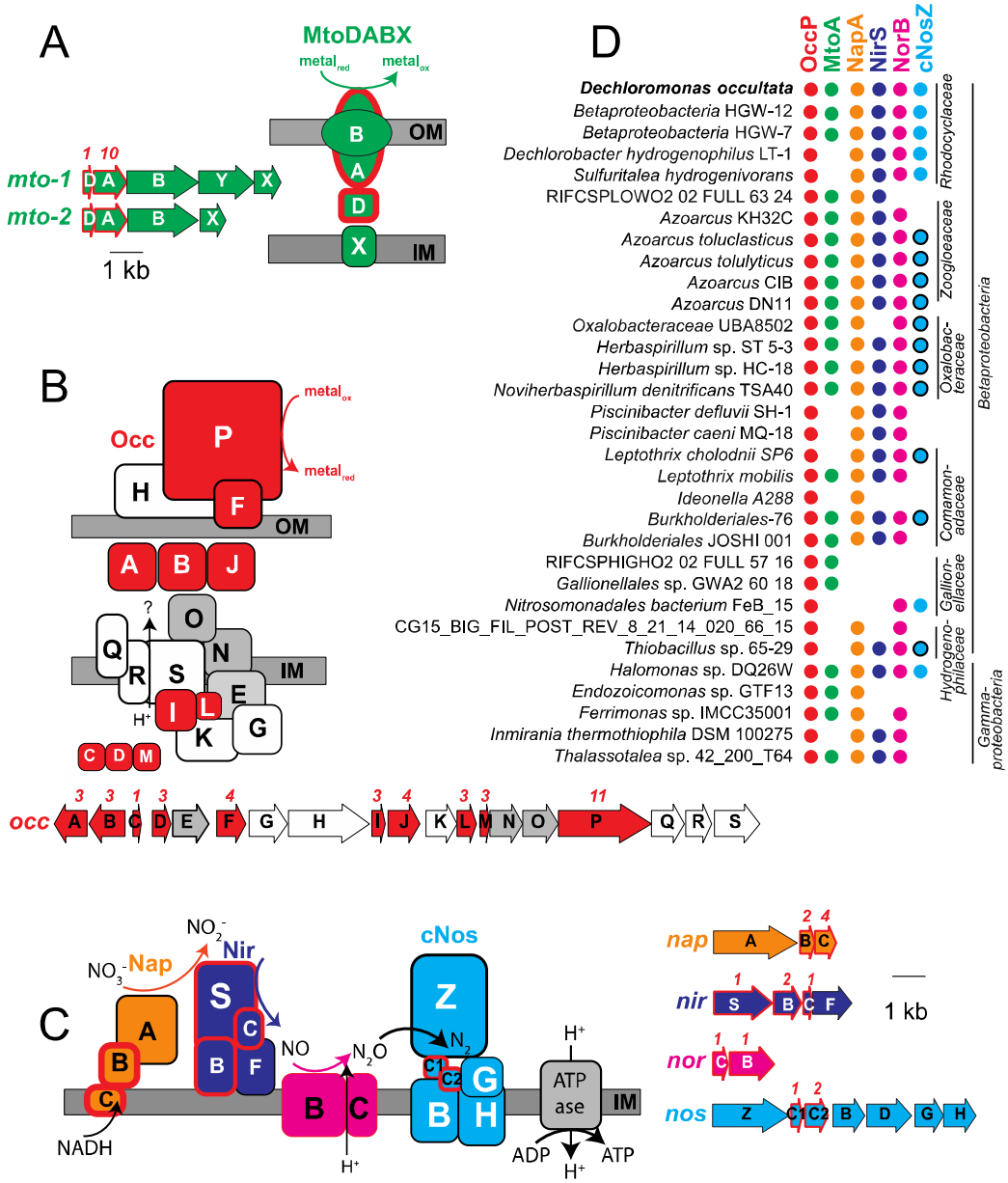

Figure 2. Gene arrangement, predicted protein location, and taxonomic distribution of major expressed respiratory complexes in "*Ca.* D. occultata". A: MtoDAB(Y)X porin-cytochrome c electron conduit; **B:** OccA-S;

C: denitrification complexes (Nap, Nir, Nor and cNos); **D:** Occurrence of key marker genes in *Betaproteobacteria* and *Gammaproteobacteria* with >95% complete genomes that encode OccP. Protein sequences from "*Ca*. D. occultata" were used as query against a genome database and searched using PSI BLAST. Matches with identities >40%, query coverage >80% and E values $<10^{-5}$ were considered positive. Red fill around genes and proteins indicate cytochrome-*c* proteins. Black outlines around blue circles in D indicate type I nitrous oxide reductase to distinguish from blue dots (type II/cytochrome-nitrous oxide reductase). Gray-shaded genes on the *occ* gene cluster indicate 6-NHL repeat proteins. Protein locations shown are based on P-sort predictions. Numbers above genes indicate number of CxxCH motifs predicted to bind cytochrome *c*. IM: inner membrane; OM: outer membrane. For more details, see **Table 1** and **Table S3.**

***Heme-copper oxidases in* "Ca. *D. occultata*".** "*Ca.* D. occultata" expressed high-affinity cbb_3-type cytochrome c oxidase (CcoNOQP) associated with microaerobic respiration (**Table S4).** Features of the "*Ca*. D. occultata" *occS* gene product, including conserved histidine residues (H-94, H-411, and H-413) that bind hemes a and a_3, as well as the H-276 residue that binds Cu_B (**Fig. S6**), suggest that OccS may function similarly to CcoN, the terminal heme-copper oxidase proton pump in aerobic respiration. All identified OccS amino acid sequences lack Cu_B ligands Y-280 and H-403, and most lack Cu_B ligands H-325 and H-326. OccS sequences also lack polar and ionizable amino acids that comprise the well-studied D and K channels involved in proton translocation in characterized cytochrome c oxidases (Blomberg and Siegbahn, 2014), but contain conserved H, C, E, D, and Y residues that may serve in alternate proton translocation pathways, similar to those recently discovered in qNOR (Gonska et al., 2018). OccS homologs were also found in *Azoarcus* spp. and deep subsurface *Betaproteobacteria* (**Fig. S6**).

Expression of denitrification proteins and possible sources of oxidized nitrogen species. Periplasmic nitrate reductase (NapA), cytochrome nitrite reductase (NirS), and type II atypical nitrous oxide reductase (cNosZ; **Fig. S7**) were highly expressed by "*Ca.* D. occultata" **(Table 1)**. Expression of the denitrification pathway was not expected because oxidized nitrogen species were not added to the medium, to which the only nitrogen supplied was 0.2 mM NH_4Cl (along with headspace N_2). Oxidized nitrogen species could result from the oxidation of NH_4Cl, but we did not find any of the canonical genes for aerobic nor anaerobic ammonia oxidation, nor did we

163 measure any ammonium oxidation in experimental bottles from the transfer used to make **Figure**
164 **1**.

165 The expression of denitrification genes is controlled by a diverse array of transcriptional
166 regulators that depend on different signals including low levels of oxygen, even in the absence of
167 nitrate (Spiro, 2012; Lin et al., 2018). The close redox potential of Mn^{3+}-pyrophosphate (~0.8 V;
168 Yamaguchi and Sawyer, 1985)) to oxidized nitrogen species (0.35-0.75 V) at circumneutral pH
169 and the lack of oxygen in the media could have induced the expression of denitrification genes
170 simultaneously with Mn(III)-reduction genes. *Gammaproteobacteria*, for example, reduce
171 Mn(III) even in the presence of nitrate (Kostka et al., 1995), and there is precedent for microbial
172 use of multiple electron acceptors, e.g. "co-respiration" of oxygen and nitrate during aerobic
173 denitrification (Chen and Strous, 2013; Ji et al., 2015).

174 Because solid-phase Mn(III) is known to chemically oxidize NH_4^+ (Aigle et al., 2017;
175 Boumaiza et al., 2018), we tested for abiotic NH_4^+ oxidation by soluble Mn(III) (1 mM).
176 Ammonium concentrations remained unchanged, and no N_2O or NO_x^- production was observed
177 (**Fig. S8**), likely because our experiments lacked solid surfaces to mediate electron transfer.
178 Similarly, N_2O levels in the headspace of our experimental bottles with Mn(III)-reducing
179 cultures were near or below the detection limit (data not shown). These findings are consistent
180 with lack of detectable ammonium oxidation by Mn(III) pyrophosphate in estuarine sediments
181 (Crowe et al., 2012).

182 ***Electron donors.*** Methane was the only electron donor added intentionally to the
183 enrichment cultures, to select for organisms that oxidize methane anaerobically. Yet, we did not
184 detect $^{13}CO_2$ after addition of $^{13}CH_4$ (**Fig. S2**). One explanation is that $^{13}CO_2$ was produced, but
185 was subsequently assimilated by other members of the microbial community such as abundant

Deltaproteobacteria **(Fig. S1)**, as observed in previous studies (Wegener et al., 2008). A filtration step included in our protocol to measure $^{13}CO_2$ would have excluded ^{13}C-enriched biomass from our analyses. Alternatively, we considered other electron donors that might have been unintentionally present in trace amounts, but sufficiently abundant to drive the observed ~300-600 μM Mn(III) reduction **(Fig. 1)**. The ethanol catabolism pathway (PQQ-dependent methanol/ethanol dehydrogenase (RIX45050), quinoprotein alcohol dehydrogenase (RIX45053), and an NAD^+-dependent aldehyde dehydrogenase-II (RIX45061)) were all highly expressed in "Ca. *D. occultata*" **(Table 1)**. Ethanol could have been introduced to the bottles during culture preparation during sterilization of bottle stoppers. Based on the stoichiometry of ethanol oxidation coupled to Mn(III) reduction:

$$2CH_3CH_2OH + 10H_2O + 5Mn(III)_2(P_2O_7)_3 \rightarrow 4HCO_3^- + 10Mn^{2+} + 24H^+ + 15(P_2O_7)^{2-}$$

150 μM ethanol would be required to reduce 600 μM of Mn(III), which equates to ~1 μL of 70% ethanol (12 M) into 100 mL culture medium. We conclude that trace contamination of ethanol was likely the major electron donor to our cultures.

It is also possible that other substrates, such as H_2 from fermentation by other microbes in the enrichment or from impurities in the headspace gas, could have supplied another source of electrons. Indeed, an NAD-reducing hydrogenase (RIX44099-100) was expressed by "*Ca*. D. occultata" (**Table 1**). Based on the stoichiometry of H_2 oxidation coupled to Mn(III) reduction:

$$H_2 + Mn(III)_2(P_2O_7)_3 \rightarrow 2H^+ + 2Mn^{2+} + 3(P_2O_7)^{2-}$$

600 μM H_2 would be required to reduce 600 μM of Mn(III). Thus, H_2 may have contributed electrons to Mn(III) reduction, but is not likely sole electron donor. A combination of ethanol, H_2, and other trace contaminants would likely have been necessary to provide enough electrons for the additional reduction of Mn(III) observed in the $^{13}CH_4$-amended cultures compared to the

209 controls lacking $^{13}CH_4$. There is precedent for other metal-reducers simultaneously using H_2 and
210 an organic electron donor (Brown et al., 2005).

211 Another trace source of organics to our cultures could have been leaching from the rubber
212 stoppers, which were black bromobutyl and pre-boiled in 0.1 N NaOH. A previous study
213 reported that organics leaked an array of n-alkanes (C_{16}–C_{34}) and unidentified organic
214 contaminants in black bromobutyl stoppers (Niemann et al., 2015). It is also conceivable that
215 trace organic was introduced as impurities in solid Mn(III) oxide powder (99% purity) used to
216 synthesize Mn(III)-pyrophosphate.

217 Finally, we considered the possibility that 0.2 mM NH_4^+, added to the cultures as a
218 nitrogen source, could have provided the electron donor, via an unknown pathway. Based on the
219 stoichiometry of NH_4^+ oxidation coupled to Mn(III) reduction:

220 $$NH_4^+ + 3H_2O + 4Mn(III)_2(P_2O_7)_3 \rightarrow NO_3^- + 8H^+ + 8Mn^{2+} + 4(P_2O_7)^{2-}$$

221 0.2 mM NH_4^+ would supply 1.6 mM electron equivalents, which is more than enough to account
222 for the observed reduction of 600 μM of Mn(III). This process could operate cryptically if the
223 oxidized products were reduced to N_2 via denitrification enzymes, such as nitrous oxide
224 reductase (cNosZ), which was one of the most abundant proteins expressed in Mn(III)-reducing
225 cultures **(Fig. 2c, Table 1).**

226 ***Carbon metabolism*.** "*Ca.* D. occultata" appeared to be growing mixotrophically. "Ca. *D.*
227 *occultata*" encoded several central metabolic pathways, including a complete TCA cycle with a
228 glyoxylate bypass, an incomplete (acetate-dependent) 3-hydroxypropionate bicycle (3-HP), a
229 modified Calvin-Benson-Bassham (CBB) pathway, and a pathway for synthesis of
230 polyhydroxybutyrate **(Fig. S11)**. In addition, "Ca. *D. occultata*" encoded genes for organic
231 carbon transport, and lactate, acetate, and propionate utilization **(Fig. S11)**. Like *D. agitata* and

D. denitrificans, the CBB pathway of "*Ca*. D. occultata" did not encode RuBisCO and sedoheptulose-1,7-bisphosphatase (SHbisPase; **Fig. S10)**; SHbisPase may be replaced by 6-phosphofructokinase and an energy-generating pyrophosphatase (RIX41248; Kleiner et al., 2012; Zorz et al., 2018). The presence of incomplete carbon fixation pathways and for organic carbon utilization pathways suggests that "Ca. *D. occultata*" relies on organic carbon to fix inorganic carbon mixotrophically. The source of this organic carbon could have been ethanol, which is converted to acetate via the pathway discussed in the previous section.

Effect of methane. Although we did not measure appreciable $^{13}CH_4$ oxidation to $^{13}CO_2$, CH_4 stimulated Mn(III) reduction and cytochrome expression in "*Ca*. D. occultata" enrichment cultures. While the specific role of CH_4 in Mn(III) reduction remains unknown, the addition of CH_4 appeared to significantly stimulate expression of many cytochrome *c* proteins, including OccABGJK, MtoD-2, and cytochrome-*c*4 and -*c*5 proteins associated with anaerobic respiration ($p < 0.05$; **Table 1; Fig. 2C**). Expression of several "*Ca*. D. occultata" proteins involved in outer membrane structure and composition - including an extracellular DUF4214 protein located next to an S-layer protein similar to those involved in manganese binding and deposition (Wang et al., 2009), a serine protease possibly involved in Fe(III) particle attachment (Burns et al., 2009), an extracellular PEP-CTERM sorting protein for protein export (Haft et al., 2006), and a Tol-Pal system for outer membrane integrity - was higher in the presence of CH_4 (**Table 1)**.

Transporters and sensors. Numerous transporters were present in the "*Ca*. D. occultata" genome, including 26 TonB-dependent siderophore transporters, 13 TRAP transporters for dicarboxylate transport, as well as ABC transporters for branched-chained amino acids and dipeptides and polypeptides (**Table S4**). "*Ca*. D. occultata" also contained a large number of environmental sensing genes: 52 bacterial hemoglobins with PAS-PAC sensors, 8 TonB-

dependent receptors, and 8 NO responsive regulators (Dnr: Crp/fr family; **Table S4**). Uniquely in "*Ca*. D. occultata", PAC-PAS sensors flanked accessory genes *nosFLY* on the *c-nosZ* operon (**Fig. S7**). Comparison of these flanking PAC-PAS sensors in "*Ca*. D. occultata" with O_2-binding sensors revealed that an arginine ~20 aa upstream from the conserved histidine as the distal pocket ligand for O_2-binding is not present in either sensor (**Fig. S11**), suggesting that the sensor may bind a different ligand, possibly NO, consistent with the placement of these genes next to cNosZ (Shimizu et al., 2015).

Nutrient storage. Active synthesis of storage polymers suggested that "*Ca*. D. occultata" was experiencing electron acceptor starvation at the time of harvesting, consistent with Mn(III) depletion in the bottles (Liu et al., 2015; Guanghuan et al., 2018). Polyphosphate-related proteins, including phosphate transporters, polyphosphate kinase, polyphosphatase, and poly-3-hydroxybutyrate synthesis machinery were detected in the proteome (**Table S4**). Polyphosphate-accumulating organisms store polyphosphates with energy generated from organic carbon oxidation during aerobic respiration or denitrification. These stored compounds are later hydrolyzed when respiratory electron acceptors for ATP production are limiting. Cyanophycin was actively synthesized for nitrogen storage.

Geobacter. "*Ca.* Geobacter occultata" expressed proteins in the TCA cycle at moderate abundance. "*Ca.* G. occultata" contained 17 multiheme c-type cytochromes, none of which were detected in the proteome. The lack of expression of electron transport and metal-reducing pathways makes it unlikely that "*Ca.* G. occultata" was solely responsible for Mn(III) reduction observed in the incubations. A periplasmic group I Ni-Fe hydrogenase (RNC64340; 91% identity to a protein (RLB64899) from *Geobacter* MAG from terrestrial hot spring sediment) and a type IV pilin (RNC67631; 10% aromatics, 87% identity to *Geobacter pickeringii* (Holmes et al.,

278 2016)) were significantly more expressed in the presence of CH_4 than N_2 in the "*Ca.* G.
279 occultata" proteome ($p < 0.05$; **Table 1**). It is possible that "*Ca.* G. occultata" transferred
280 electrons to "*Ca*. D. occultata" via e-pilins (e.g. direct interspecies electron transfer),
281 contributing to the higher rates of Mn(III) reduction in the presence of CH_4 vs. N_2. The possible
282 involvement of *Geobacter* e-pilins in Mn(III) reduction remains an open question, due to the lack
283 of studies examining the possibility of Mn(III) reduction in *Deltaproteobacteria*.

284 ***Conclusions.*** To our knowledge, this study provides the first evidence for biological
285 reduction of soluble Mn(III) by a bacterium outside of the *Gammaproteobacteria* class. The
286 dominant bacterium in Mn(III)-reducing enrichment cultures was "*Ca*. D. occultata", a member
287 of the *Rhodocyclales* order of *Betaproteobacteria*. "*Ca*. D. occultata" expressed decahemes
288 similar to the Mto pathway, and *occ* genes, including a novel extracellular undecaheme (OccP),
289 which are predicted to encode a new respiratory electron transport pathway. The novel *occ*
290 operon was found to be widespread in *Betaproteobacteria* from the deep subsurface, where metal
291 cycling can fuel microbial metabolism. We also found highly expressed peptides from various
292 central metabolic cycles and organic substrate utilization pathways, suggesting that "Ca. *D.*
293 *occultata*" may have been using multiple pathways simultaneously for energy generation and
294 carbon assimilation during Mn(III) reduction.

295 Puzzles remain about whether "*Ca*. D. occultata" can transform two potent greenhouse
296 gases: methane and nitrous oxide. Although "*Ca*. D. occultata" was enriched with CH_4 as the
297 sole electron donor and cultures reduced Mn(III) more rapidly in the presence of CH_4, no CH_4
298 oxidation activity was measured in Mn(III)-reducing cultures, and proteomic data suggested that
299 "*Ca*. D. occultata" was growing mixotrophically rather than assimilating CH_4. Further, although
300 we did not add oxidized nitrogen compounds to our media, and Mn(III) did not chemically

oxidize NH_4^+ under our culture conditions, type II nitrous oxide reductase (cNosZ) was one of the most abundant proteins expressed in Mn(III)-reducing cultures. The role of cNosZ and other denitrification enzymes in "*Ca*. D. occultata" metabolism, and their possible connection to Mn(III) reduction, remain to be investigated.

Acknowledgements. This research was funded by NASA Exobiology grant NNX14AJ87G. Support was also provided by a Center for Dark Energy Biosphere Investigations (NSF-CDEBI OCE-0939564) small research grant and supported by the NASA Astrobiology Institute (NNA15BB03A) and a NASA Astrobiology Postdoctoral Fellowship to NS. SAC was supported through NSERC CRC, CFI, and Discovery grants. We thank Marcus Bray, Andrew Burns, Caleb Easterly, Ellery Ingall, Pratik Jagtap, Cory Padilla, Angela Peña, Johnny Striepen, Yael Toporek, and Rowan Wolschleger for technical assistance. We thank Karen Lloyd, Nagissa Mahmoudi, and Emily Weinert for helpful discussions.

Competing Interests: The authors declare no competing interests.

316 **Table 1. Expression levels for select "*Ca*. Dechloromonas occultata" and "*Ca*. Geobacter occultata" proteins**
317 **in the presence of CH_4 and N_2.** Gray boxes indicate membrane proteins[1]. Bold proteins indicate proteins that were
318 significantly more expressed with CH_4 than N_2 ($CH_4/N_2>1$; $p<0.05$). P values indicate significance of abundance
319 difference between CH_4 and N_2 treatments.

[1]SP: signal peptide (Y:present/N:absent); TMH: numbers of transmembrane helices; CxxCH: number of heme-binding motifs; P-sort: predicted cellular location based on Psortb v.3.0. MCP: methyl-accepting chemotaxis protein; PPIase: Peptidyl-proline isomerase; P: periplasm, C: cytoplasm; OM: outer membrane; IM: inner membrane, E: extracellular; U: unknown. MtoX and MtoY were predicted to be an inner membrane cytochrome-b protein and a methyl-accepting chemotaxis protein, respectively. Membrane proteins may be underrepresented by mass spectrometry-based metaproteomic analyses, which inherently favor soluble over insoluble membrane-bound or hydrophobic proteins.

Protein Sequence Predictions								Normalized Peptide Abundance						
Enzyme Complex/ Category	Function	Proteins	NCBI ID	Motifs				By Treatment				Differential Peptide		
				SP	TMH	CxxCH	P-sort	CH_4	SD	N_2	SD	Avg	SD	P value
Ca. Dechloromonas occultata														
Mtc-1	Outer membrane porin-cytochrome c electron conduit	MtoX-1 (cyt-b)	RIX49676	N	5	0	IM							
		MtoY-1 (MCP)	RIX49677	N	2	1	IM	2.7	0.5	3.6	0.2	0.8	0.2	0.2
		MtoB-1 (porin)	RIX49678	Y	0	0	OM	10	2	15	2	0.6	0.1	0.004
		MtoA-1	RIX49874	Y	1	10	P	5	1	2.5	0.1	1.9	0.4	0.1
		MtoD-1	RIX49875	N	0	1	P							
Mtc-2	Outer membrane porin-cytochrome c electron conduit	MtoX-2 (cyt-b)	RIX48942	N	4	0	IM							
		MtoB-2 (porin)	RIX48943	Y	0	0	OM	8	1	16	0.2	0.5	0.1	0.04
		MtoA-2	RIX48944	Y	1	10	P	7.3	0.8	4	2	2.1	1.3	0.2
		MtoD-2	**RIX48945**	**Y**	**1**	**1**	**U**	**2.6**	**0.3**	**0.7**	**0.3**	**4.0**	**1.4**	**0.003**
Occ	Membrane-spanning electron transport cytochromes	**OccA**	**RIX49688**	**Y**	**1**	**3**	**P**	**4**	**0.5**	**0.7**	**0.6**	**7.8**	**5.7**	**0.01**
		OccB	**RIX49689**	**Y**	**0**	**3**	**U**	**41**	**4**	**19**	**2**	**2.2**	**0.0**	**0.03**
		OccC	RIX49877	N	0	1	U							
		OccD	RIX49878	N	0	3	U							
		OccE (6-NHL)	RIX49690	N	1	0	U	22	2.1	20.5	0.2	1.1	0.1	0.2
		OccF	RIX49691	Y	2	4	E	13	0.7	10.1	0.1	1.3	0.1	0.06
		OccG (PPIase)	**RIX49692**	**N**	**0**	**0**	**U**	**14**	**1**	**3.3**	**0.5**	**4.2**	**0.3**	**0.01**
		OccH	RIX49693	N	0	0	OM/E	6.0	0.2	7.7	0.6	0.8	0.1	0.10
		OccI	RIX49694	N	1	3	U	7	2.5	2.3	0.0	2.9	1.1	0.1
		OccJ	**RIX49879**	**Y**	**0**	**4**	**U**	**44**	**0.2**	**19**	**3**	**2.4**	**0.4**	**0.03**
		OccK	**RIX49880**	**N**	**0**	**0**	**C**	**39**	**6**	**13**	**1**	**3.0**	**0.2**	**0.04**
		OccL	RIX49695	N	1	3	U							
		OccM	RIX49881	N	0	3	U							
		OccN (6 NHL)	RIX49696	N	2	0	U	5.7	0.3	6	1	0.9	0.1	0.2
		OccO (6 NHL)	RIX49882	N	0	0	U	1.2	0.8	4.2	0.4	0.3	0.2	0.03
		OccP	RIX49697	N	0	11	E	14	2	12	3	1.2	0.5	0.4
		OccQ	RIX49698	Y	4	0	IM							
		OccR	RIX49883	N	8	0	IM							
		OccS	RIX49699	N	12	0	IM							
Cyt c	Mono- and diheme c-type cytochromes involved in electron transfer	**Cyt c5**	**RIX47670**	**N**	**1**	**1**	**U**	**27**	**2**	**9**	**3**	**3.2**	**0.8**	**0.01**
		Cyt c5	RIX40984	Y	1	2	P	19	2	6	1	**3.3**	**1.0**	0.06
		Cyt c'/C_2	RIX44710	Y	1	1	P	17	5	3.6	0.8	**4.8**	**2.3**	0.09
		Cyt c'/C_2	RIX49630	Y	1	1	P	7	1	1.2	0.9	**8.2**	**6.6**	0.07
		Cyt c551/c552	RIX49087	Y	0	1	P	13	3	2.8	0.0	**4.8**	**1.1**	0.06
		Cyt c4	RIX48804	Y	0	2	P	16	0.8	9.8	0.8	**1.6**	**0.2**	0.06
		Cyt c4	RIX44782	Y	0	2	P	4	2	1.7	0.7	**2.6**	**0.1**	0.08
		Cyt c4	**RIX45018**	**Y**	**0**	**2**	**P**	**7**	**0.6**	**2.2**	**0.2**	**3.0**	**0.0**	**0.02**
Nap	Periplasmic nitrate reductase	NapA	RIX41011	Y	0	0	P	76	2	67	3	1.1	0.1	0.1
		NapB	**RIX41010**	**Y**	**1**	**2**	**P**	**15**	**1**	**5**	**2**	**3.2**	**0.9**	**0.02**
		NapC	RIX41009	N	1	4	IM	12	3	13	1	1.0	0.2	0.1
Nir	Nitrite reductase	NirS	RIX44719	Y	0	1	P	58	2	44	4	1.3	0.2	0.1
		NirB	RIX44720	Y	1	2	P	14	3	10	2	1.5	0.6	0.2
		NirC	RIX44788	N	0	1	P							
		NirF	RIX44721	Y	1	0	P or C	2	1	7	1	0.3	0.1	0.02
Nor	Nitric oxide reductase	NorC	RIX45182	N	1	1	IM	3.5	0.7	3.2	0.7	1.1	0.0	0.1
		NorB	RIX45183	N	12	1	IM							
cNos	Type II nitrous oxide reductase	cNosZ	RIX42539	Y	0	0	P	77	17	66	8	1.2	0.3	0.2
		cNosC1	RIX42538	Y	1	1	P	16	2	4	2	4.9	3.3	0.08
		cNosC2	**RIX42537**	**Y**	**1**	**2**	**P**	**10**	**0.1**	**3.9**	**0.3**	**2.6**	**0.1**	**0.02**
		cNosB	RIX42536	N	6	0	IM							
		cNosD	RIX42535	N	0	0	P							
		cNosG	RIX42534	N	1	0	C							
		cNosH	RIX42533	N	4	0	IM							
Qcr	Menaquinol-cytochrome c reductase complex	QcrA	RIX41976	N	9	0	CM							
		QcrB	RIX41977	N	9	0	CM							
		QcrC	RIX41978	N	1	0	CM							
Proteases	Serine protease		**RIX49468**	**N**	**0**	**0**	**P**	**27**	**2**	**1.0**	**0.3**	**29.0**	**9.9**	**0.02**
	Carboxyl-terminal protease (S41)		**RIX48818**	**N**	**1**	**0**	**CM**	**18.5**	**0.8**	**8.0**	**0.9**	**2.3**	**0.1**	**0.0002**
Membrane/Extracellular	DUF4214 protein		**RIX44180**	**N**	**0**	**0**	**OM/E**	**146**	**25**	**43**	**0.6**	**3.4**	**0.5**	**0.05**
	S-layer protein		RIX44181	N	0	0	U	8	0.5	10	0.6	0.8	0.1	0.14
	PEP-CTERM sorting protein		**RIX45463**	**Y**	**1**	**0**	**E**	**68**	**6**	**33**	**10**	**2.1**	**0.5**	**0.03**
	Tol-Pal system protein	TolB	**RIX44015**	**Y**	**0**	**0**	**P**	**20**	**2**	**12**	**1**	**1.7**	**0.0**	**0.03**
	Peptidoglycan-associated lipoprotein	Pal	**RIX44016**	**N**	**0**	**0**	**OM**	**27.3**	**0.2**	**10**	**3**	**2.7**	**0.7**	**0.04**
	Tol-Pal system protein	YbgF	RIX44017	Y	0	0	U	10.8	0.4	4	2	3.7	2.2	0.06
	Pilus assembly protein		**RIX46961**	**N**	**0**	**0**	**U**	**54**	**5**	**30**	**5**	**1.8**	**0.1**	**0.001**
Other	Ethanol/methanol dehydrogenase		**RIX45050**	**Y**	**0**	**0**	**P**	**37**	**4**	**17**	**1**	**2.2**	**0.1**	**0.03**
	Alcohol dehydrogenase		RIX45053	Y	0	0	P	12.4	1.4	14.2	1.7	0.9	0.0	0.04
	Aldehyde dehydrogenase		RIX45061	Y	0	0	P	125	31	221	75	0.6	0.1	0.10
	Phasin family granule-associated protein		**RIX40682**	**N**	**0**	**0**	**U**	**49**	**2**	**22**	**1**	**2.2**	**0.2**	**0.03**
	Phasin family granule-associated protein		**RIX40683**	**Y**	**0**	**0**	**U**	**34**	**4**	**16**	**1**	**2.1**	**0.0**	**0.03**
	High potential iron-sulfur protein		**RIX49681**	**Y**	**0**	**0**	**U**	**10.79**	**0.01**	**6.5**	**0.4**	**1.7**	**0.1**	**0.02**
	Electron transfer flavoprotein	FixA	**RIX43544**	**N**	**0**	**0**	**C**	**16**	**3**	**10**	**2**	**1.7**	**0.0**	**0.04**
	NAD-reducing hydrogenase	HoxH	RIX46736	N	0	0	C	22.9	0.7	37	3	0.6	0.1	0.07
Ca. Geobacter occultata														
Hydrogenase	[Ni/Fe] hydrogenase, group 1, small subunit	HyaA	RNC64339	Y	0	0	P	11.1	0.4	3	1	5	2	0.06
	[Ni/Fe] hydrogenase, group 1, large subunit	**HyaB**	**RNC64340**	**N**	**0**	**0**	**P**	**32**	**0**	**11**	**5**	**3**	**1**	**0.01**
E-pilus	Type IV pilin	**PilA**	**RNC67631**	**N**	**1**	**0**	**E**	**93**	**3**	**18**	**3**	**5.6**	**0.6**	**0.02**

References

Aigle, A., Bonin, P., Iobbi-Nivol, C., Mejean, V., and Michotey, V. (2017) Physiological and transcriptional approaches reveal connection between nitrogen and manganese cycles in Shewanella algae C6G3. *Sci Rep* **7**: 44725.

Anantharaman, K., Brown, C.T., Hug, L.A., Sharon, I., Castelle, C.J., Probst, A.J. et al. (2016) Thousands of microbial genomes shed light on interconnected biogeochemical processes in an aquifer system. *Nat Commun* **7**: 13219.

328 Beal, E.J., House, C.H., and Orphan, V.J. (2009) Manganese- and iron-dependent marine methane
329 oxidation. *Science* **325**: 184-187.

330 Blomberg, M.R., and Siegbahn, P.E. (2014) Proton pumping in cytochrome c oxidase: Energetic
331 requirements and the role of two proton channels. *Biochim Biophys Acta* **1837**: 1165-1177.

332 Boumaiza, H., Coustel, R., Despas, C., Ruby, C., and Bergaoui, L. (2018) Interaction of ammonium with
333 birnessite: Evidence of a chemical and structural transformation in alkaline aqueous medium. *J Solid*
334 *State Chem* **258**: 543-550.

335 Brown, D.G., Komlos, J., and Jaffé, P.R. (2005) Simultaneous utilization of acetate and hydrogen by
336 Geobacter sulfurreducens and implications for use of hydrogen as an indicator of redox conditions.
337 *Environmental science & technology* **39**: 3069-3076.

338 Burns, J.L., Ginn, B.R., Bates, D.J., Dublin, S.N., Taylor, J.V., Apkarian, R.P. et al. (2009) Outer
339 membrane-associated serine protease involved in adhesion of *Shewanella oneidensis* to Fe(III) oxides.
340 *Environ Sci Technol* **44**: 68-73.

341 Chen, J., and Strous, M. (2013) Denitrification and aerobic respiration, hybrid electron transport chains
342 and co-evolution. *Biochimica et Biophysica Acta (BBA)-Bioenergetics* **1827**: 136-144.

343 Crowe, S.A., Canfield, D.E., Mucci, A., Sundby, B., and Maranger, R. (2012) Anammox, denitrification
344 and fixed-nitrogen removal in sediments from the Lower St. Lawrence Estuary. *Biogeosciences* **9**: 4309-
345 4321.

346 Crowe, S.A., O'Neill, A.H., Katsev, S., Hehanussa, P., Haffner, G.D., Sundby, B. et al. (2008) The
347 biogeochemistry of tropical lakes: A case study from Lake Matano, Indonesia. *Limnology and*
348 *Oceanography* **53**: 319-331.

349 Crowe, S.A., Katsev, S., Leslie, K., Sturm, A., Magen, C., Nomosatryo, S. et al. (2011) The methane
350 cycle in ferruginous Lake Matano. *Geobiology* **9**: 61-78.

351 Cummings, D.E., Caccavo, F., Spring, S., and Rosenzweig, R.F. (1999) Ferribacterium limneticum, gen.
352 nov., sp. nov., an Fe(III)-reducing microorganism isolated from mining-impacted freshwater lake
353 sediments. *Arch Microbiol* **171**: 183-188.

354 Diem, D., and Stumm, W. (1984) Is dissolved Mn2+ being oxidized by O2 in absence of Mn-bacteria or
355 surface catalysts? *Geochimica et Cosmochimica Acta* **48**: 1571-1573.

356 Edwards, M.J., Hall, A., Shi, L., Fredrickson, J.K., Zachara, J.M., Butt, J.N. et al. (2012) The crystal
357 structure of the extracellular 11-heme cytochrome UndA reveals a conserved 10-heme motif and defined
358 binding site for soluble iron chelates. *Structure* **20**: 1275-1284.

359 Emerson, D., Field, E.K., Chertkov, O., Davenport, K.W., Goodwin, L., Munk, C. et al. (2013)
360 Comparative genomics of freshwater Fe-oxidizing bacteria: implications for physiology, ecology, and
361 systematics. *Front Microbiol* **4**: 254.

362 Ettwig, K.F., Zhu, B., Speth, D., Keltjens, J.T., Jetten, M.S.M., and Kartal, B. (2016) Archaea catalyze
363 iron-dependent anaerobic oxidation of methane. *Proceedings of the National Academy of Sciences* **113**:
364 12792-12796.

365 Finneran, K.T., Johnsen, C.V., and Lovley, D.R. (2003) *Rhodoferax ferrireducens* sp. nov., a
366 psychrotolerant, facultatively anaerobic bacterium that oxidizes acetate with the reduction of Fe(III). *Int J*
367 *Syst Evol Microbiol* **53**: 669-673.

368 Fredrickson, J.K., Romine, M.F., Beliaev, A.S., Auchtung, J.M., Driscoll, M.E., Gardner, T.S. et al.
369 (2008) Towards environmental systems biology of *Shewanella*. *Nat Rev Microbiol* **6**: 592.

370 Gonska, N., Young, D., Yuki, R., Okamoto, T., Hisano, T., Antonyuk, S. et al. (2018) Characterization of
371 the quinol-dependent nitric oxide reductase from the pathogen *Neisseria meningitidis*, an electrogenic
372 enzyme. *Sci Rep* **8**: 3637.

373 Guanghuan, G., Jianqiang, Z., Aixia, C., Bo, H., Ying, C., Kun, G. et al. (2018) Nitrogen removal and
374 nitrous oxide emission in an anaerobic/oxic/anoxic sequencing biofilm Batch reactor. *Environ Eng Sci* **35**:
375 19-26.

376 Haft, D.H., Paulsen, I.T., Ward, N., and Selengut, J.D. (2006) Exopolysaccharide-associated protein
377 sorting in environmental organisms: the PEP-CTERM/EpsH system. Application of a novel phylogenetic
378 profiling heuristic. *BMC Biol* **4**: 29.

379 He, S., Barco, R.A., Emerson, D., and Roden, E.E. (2017) Comparative genomic analysis of neutrophilic
380 iron(II) oxidizer genomes for candidate genes in extracellular electron transfer. *Front Microbiol* **8**: 1584.

381 Heintze, S., and Mann, P. (1947) Soluble complexes of manganic manganese. *J Agric Sci* **37**: 23-26.

382 Hem, J.D. (1963) *Chemical equilibria and rates of manganese oxidation*: US Government Printing
383 Office.

384 Hernsdorf, A.W., Amano, Y., Miyakawa, K., Ise, K., Suzuki, Y., Anantharaman, K. et al. (2017) Potential
385 for microbial H2 and metal transformations associated with novel bacteria and archaea in deep terrestrial
386 subsurface sediments. *ISME J* **11**: 1915-1929.

387 Holmes, D.E., Dang, Y., Walker, D.J., and Lovley, D.R. (2016) The electrically conductive pili of
388 *Geobacter* species are a recently evolved feature for extracellular electron transfer. *Microb Genom* **2**.

389 Ji, B., Yang, K., Zhu, L., Jiang, Y., Wang, H., Zhou, J., and Zhang, H. (2015) Aerobic denitrification: a
390 review of important advances of the last 30 years. *Biotechnology and bioprocess engineering* **20**: 643-
391 651.

392 Jones, C., Crowe, S.A., Sturm, A., Leslie, K.L., MacLean, L.C.W., Katsev, S. et al. (2011)
393 Biogeochemistry of manganese in ferruginous Lake Matano, Indonesia. *Biogeosciences* **8**: 2977-2991.

394 Jung, H., Taillefert, M., Sun, J., Wang, Q., Borkiewicz, O.J., Liu, P. et al. (2020) Redox Cycling Driven
395 Transformation of Layered Manganese Oxides to Tunnel Structures. *Journal of the American Chemical*
396 *Society*.

397 Kato, S., Ohkuma, M., Powell, D.H., Krepski, S.T., Oshima, K., Hattori, M. et al. (2015) Comparative
398 Genomic Insights into Ecophysiology of Neutrophilic, Microaerophilic Iron Oxidizing Bacteria. *Front*
399 *Microbiol* **6**: 1265.

Kleiner, M., Wentrup, C., Lott, C., Teeling, H., Wetzel, S., Young, J. et al. (2012) Metaproteomics of a gutless marine worm and its symbiotic microbial community reveal unusual pathways for carbon and energy use. *Proc Natl Acad Sci* **109**: 1173-1182.

Kostka, J.E., Luther, G.W., and Nealson, K.H. (1995) Chemical and biological reduction of Mn(III)-pyrophosphate complexes - potential importance of dissolved Mn(III) as an environmental oxidant. *Geochim Cosmochim Acta* **59**: 885-894.

Kuntz, L.B., Laakso, T.A., Schrag, D.P., and Crowe, S.A. (2015) Modeling the carbon cycle in Lake Matano. *Geobiology* **13**: 454-461.

Learman, D., Wankel, S., Webb, S., Martinez, N., Madden, A., and Hansel, C. (2011) Coupled biotic–abiotic Mn (II) oxidation pathway mediates the formation and structural evolution of biogenic Mn oxides. *Geochem Cosmochim Acta* **75**: 6048-6063.

Leu, A.O., Cai, C., McIlroy, S.J., Southam, G., Orphan, V.J., Yuan, Z. et al. (2020) Anaerobic methane oxidation coupled to manganese reduction by members of the Methanoperedenaceae. *The ISME Journal* **14**: 1030-1041.

Lin, Y.-C., Sekedat, M.D., Cornell, W.C., Silva, G.M., Okegbe, C., Price-Whelan, A. et al. (2018) Phenazines Regulate Nap-Dependent Denitrification in Pseudomonas aeruginosa Biofilms. *Journal of Bacteriology* **200**: e00031-00018.

Liu, Y., Peng, L., Guo, J., Chen, X., Yuan, Z., and Ni, B.-J. (2015) Evaluating the role of microbial internal storage turnover on nitrous oxide accumulation during denitrification. *Sci Rep* **5**: 15138.

Luther, G.W., Thibault de Chanvalon, A., Oldham, V.E., Estes, E.R., Tebo, B.M., and Madison, A.S. (2018) Reduction of Manganese Oxides: Thermodynamic, Kinetic and Mechanistic Considerations for One- Versus Two-Electron Transfer Steps. *Aquatic Geochemistry* **24**: 257-277.

Luther III, G.W., Madison, A.S., Mucci, A., Sundby, B., and Oldham, V.E. (2015) A kinetic approach to assess the strengths of ligands bound to soluble Mn (III). *Marine Chemistry* **173**: 93-99.

Madison, A.S., Tebo, B.M., Mucci, A., Sundby, B., and Luther, G.W., 3rd (2013) Abundant porewater Mn(III) is a major component of the sedimentary redox system. *Science* **341**: 875-878.

Morgan, J.J. (2005) Kinetics of reaction between O2 and Mn (II) species in aqueous solutions. *Geochimica et Cosmochimica Acta* **69**: 35-48.

Niemann, H., Steinle, L., Blees, J., Bussmann, I., Treude, T., Krause, S. et al. (2015) Toxic effects of lab□grade butyl rubber stoppers on aerobic methane oxidation. *Limnol Oceangr: Methods* **13**: 40-52.

Oldham, V.E., Siebecker, M.G., Jones, M.R., Mucci, A., Tebo, B.M., and Luther, G.W. (2019) The speciation and mobility of Mn and Fe in estuarine sediments. *Aquat Geochem* **25**: 3-26.

Richardson, D.J., Butt, J.N., Fredrickson, J.K., Zachara, J.M., Shi, L., Edwards, M.J. et al. (2012) The 'porin–cytochrome' model for microbe□to□mineral electron transfer. *Mol Microbiol* **85**: 201-212.

435 Riedinger, N., Formolo, M.J., Lyons, T.W., Henkel, S., Beck, A., and Kasten, S. (2014) An inorganic
436 geochemical argument for coupled anaerobic oxidation of methane and iron reduction in marine
437 sediments. *Geobiology* **12**: 172-181.

438 Shi, L., Belchik, S.M., Wang, Z., Kennedy, D.W., Dohnalkova, A.C., Marshall, M.J. et al. (2011)
439 Identification and characterization of UndAHRCR-6, an outer membrane endecaheme c-type cytochrome
440 of *Shewanella* sp. strain HRCR-6. *Appl Environ Microbiol* **77**: 5521-5523.

441 Shi, L., Dong, H., Reguera, G., Beyenal, H., Lu, A., Liu, J. et al. (2016) Extracellular electron transfer
442 mechanisms between microorganisms and minerals. *Nat Rev Microbiol* **14**: 651.

443 Shimizu, T., Huang, D., Yan, F., Stranava, M., Bartosova, M., Fojtíková, V., and Martínková, M.t. (2015)
444 Gaseous O2, NO, and CO in signal transduction: structure and function relationships of heme-based gas
445 sensors and heme-redox sensors. *Chem Rev* **115**: 6491-6533.

446 Smith, J.A., Lovley, D.R., and Tremblay, P.L. (2013) Outer cell surface components essential for Fe(III)
447 oxide reduction by Geobacter metallireducens. *Appl Environ Microbiol* **79**: 901-907.

448 Spiro, S. (2012) Nitrous oxide production and consumption: regulation of gene expression by gas-
449 sensitive transcription factors. *Philosophical transactions of the Royal Society of London Series B,*
450 *Biological sciences* **367**: 1213-1225.

451 Sturm, A., Fowle, D.A., Jones, C., Leslie, K., Nomosatryo, S., Henny, C. et al. (2019) Rates and
452 pathways of CH4 oxidation in ferruginous Lake Matano, Indonesia. *Geobiology* **17**: 294-307.

453 Szeinbaum, N., Burns, J.L., and DiChristina, T.J. (2014) Electron transport and protein secretion
454 pathways involved in Mn(III) reduction by Shewanella oneidensis. *Environ Microbiol Rep* **6**: 490-500.

455 Szeinbaum, N., Lin, H., Brandes, J.A., Taillefert, M., Glass, J.B., and DiChristina, T.J. (2017) Microbial
456 manganese(III) reduction fuelled by anaerobic acetate oxidation. *Environ Microbiol* **19**: 3475-3486.

457 Tebo, B.M., Johnson, H.A., McCarthy, J.K., and Templeton, A.S. (2005) Geomicrobiology of
458 manganese(II) oxidation. *Trends Microbiol* **13**: 421-428.

459 Wang, X., Schröder, H.C., Schloßmacher, U., and Müller, W.E. (2009) Organized bacterial assemblies in
460 manganese nodules: evidence for a role of S-layers in metal deposition. *Geo-Marine Letters* **29**: 85-91.

461 Wegener, G., Niemann, H., Elvert, M., Hinrichs, K.U., and Boetius, A. (2008) Assimilation of methane
462 and inorganic carbon by microbial communities mediating the anaerobic oxidation of methane. *Environ*
463 *Microbiol* **10**: 2287-2298.

464 Yamaguchi, K.S., and Sawyer, D.T. (1985) The redox chemistry of manganese(III) and manganese(IV)
465 complexes. *Isr J Chem* **25**: 164-176.

466 Yang, Y., Chen, J., Qiu, D., and Zhou, J. (2013) Roles of UndA and MtrC of *Shewanella putrefaciens*
467 W3-18-1 in iron reduction. *BMC Microbiol* **13**: 267.

468 Zorz, J.K., Kozlowski, J.A., Stein, L.Y., Strous, M., and Kleiner, M. (2018) Comparative proteomics of
469 three species of ammonia-oxidizing bacteria. *Front Microbiol* **9**: 938.

470

471